

Choice of the Definition Method for the Total Electron Content to Describe the Conditions in the Ionosphere

Olga Maltseva

*Institute of Physics Southern Federal University, Stachki, 194, Rostov-on-Don, Russia
mal@ip.rsu.ru*

Keywords: GPS. Total electron content TEC. Ionospheric models. Radio wave propagation. Geomagnetic disturbances.

Abstract: Conditions of radio-wave propagation in the ionosphere, influencing functioning of the modern navigation and communication systems, are defined by the critical frequency foF2 and an electron density distribution termed the N(h)- profile. In the given paper, the experimental values of the total electron content TEC(obs) are used for their determination. It is shown that the median of the equivalent slab thickness of the ionosphere is the good calibration factor, allowing to obtain values of foF2 from TEC(obs) of any global map though in most cases values of foF2, the closest to foF2(obs), are provided with the JPL map. For coordination of the N(h)-profile with values of TEC(obs), coefficient K(PL), modifying a plasmaspheric part of a profile, is entered (up to heights of navigation and geostationary satellites). In this case, the CODE map is the best one. It is necessary to have models of the TEC parameter to support navigation system operation. It is shown that the big progress in modeling of this parameter is reached during the last years: appearance of various models allows us to compare and use them at forecast TEC for any level of solar activity. It is especially important, because values of solar spots and the F10.7 parameter and also geomagnetic indexes of Kp, Dst, AE are well enough predicted.

1 INTRODUCTION

The ionosphere plays an important role in the life of mankind: it mitigates the blows of solar wind and provides wave propagation of various frequency bands. The systems connected to the ionosphere are most full presented in Tab. 1 from the paper (Goodman, 2005).

Category 1 involves those systems that depend upon the ionosphere (i.e., involve the ionosphere as part of the system), and category 2 involves those systems for which the ionosphere is simply a nuisance. The special role for description of the ionospheric conditions is played by models, and the model, capable to provide high accuracy of description of ionospheric characteristic distribution, should be adapted for the experimental information in a real time mode.

Table 1: Categories of radio systems in terms of ionospheric dependence

Category 1: systems that depend upon the ionosphere	Category 2: systems for which the ionosphere is simply a nuisance
VLF-LF communication and navigation	Satellite communication
MF communication	Satellite navigation (e.g., GPS&GLONASS)
HF communication	Space-based radar and imaging
HF broadcasting (“short-wave” listening)	Terrestrial radar surveillance and tracking
OTH radar surveillance	Meteor-burst communication
HFDF and HF SIGINT	Any other system for which the ionosphere is not necessary for conveyance

The data which can be used in such an approach should be available and operatively updated.

Traditional parameters meeting such requirements are the critical frequency foF2 and maximum height hmF2. Because the total electron content TEC is the most important parameter of the ionosphere for the operation of technological systems, in the given paper it is used for this purpose. TEC data are available and is updated in several Internet archives. From huge number of possible applications of TEC, in the present paper the preference is given for an estimation of possibility of determination of propagation conditions. It means usage of TEC for determination of foF2 (or too NmF2) and N(h)- profiles. The huge need exists in the forecast of these parameters, and, hence, of TEC. It is possible to select three methods of the TEC determination: (1) measurements, (2) empirical modeling, (3) integration of theoretical or empirical N(h)-profiles. Information and results are given for each of these methods.

2 MEASUREMENT METHODS

The most widespread are global maps JPL, CODE, UPC, ESA, created by Jet Propulsion Laboratory of California Institute of Technology (Pasadena, USA), the Center for Orbit Determination in Europe (CODE) of the International GPS Service for Geodynamics (Switzerland), Astronomy and Geomatics of the Polytechnical University of Catalonia, Barcelona, Spain (UPC), European Space Agency (Germany) respectively as TEC experimental data (e.g. Schaer et al., 1995; Mannucci et al., 1998; Hernandez-Pajares et al., 1997; Sardon et al., 1994; Jakowski et al., 1996). For specific coordinates and time, the maps can be derived from the IONEX (IONosphere map Exchange) files (<ftp://cdis.gsfc.nasa.gov/pub/gps/products/ionex/>). Owing to the big differences of methods (on determination of biases, approximating functions, etc.), values of TEC for various maps and other methods of determination TEC are strongly differed. Traditional examples of such differences are Figures from the paper (Arikan et al., 2003).

Now, the GPS community selected the average IGS values as the standard (Hernandez et al., 2009), therefore in the given paper all maps, including IGS, are used. These maps are given on the same site and already start to be used, e.g. (Lean et al., 2011). We use all maps for comparison. However, under the valid remark of (Lastovicka, 2013), such selection does not remove the restrictions inherent in each

method. JPL is used in paper (Gulyaeva and Stanislawski, 2008), CODE is used in paper (Jakowski et al., 2006). Other methods also yield comparable results.

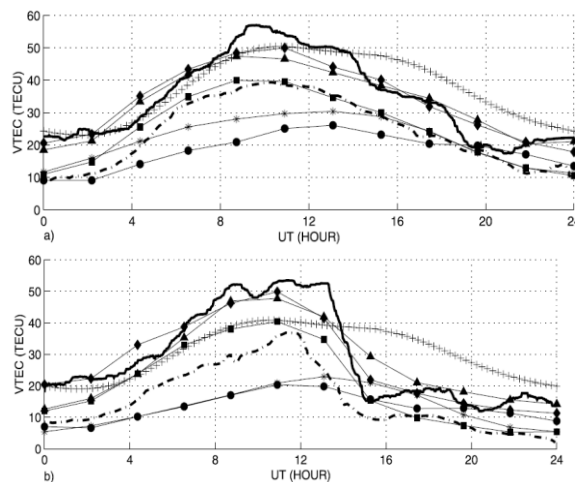


Figure 1: Comparison of the estimated TEC values from the algorithm with other models of TEC for Kiruna, estimated VTEC from the developed algorithm (solid line), RCRU (dashed line), IRI model (pluses), gAGE/UPC (triangles and a solid line), JPL-GNISD (diamonds and a solid line), ESA/ESOC (circles and a solid line), NRCAN (stars and a solid line), CODE (squares and a solid line). (a) 25 April 2001 and (b) 28 April 2001.

3 METHODS OF EMPIRICAL MODELING

Empirical modeling plays an important role both for the forecast of ionospheric parameters, and for validation of models. For modeling of TEC, basically, the method of orthogonal components is used (Zhang et al., 2012; Ivanov et al., 2011), however authors do not give appropriate coefficients and functions. Besides, there is a difficulty of the forecast at an output for temporal boundaries of the used data, therefore the main attention is given for available and new models. Many long years, the most simple model of Klobuchar (Klobuchar, 1987) was unique for adjustment of delay of signals in the ionosphere and till now is widely used for systems with single-frequency receivers though the authors using it note a row of shortcomings, for example (Chen and Gao, 2005). The model (Kakinami, 2009) is an example of models for specific station which should possess the high accuracy. The model is based on values of the instrumental biases given by the JPL laboratory. Results of the test of this model

in the form of correspondence between model and experimental values are given on Fig. 2.

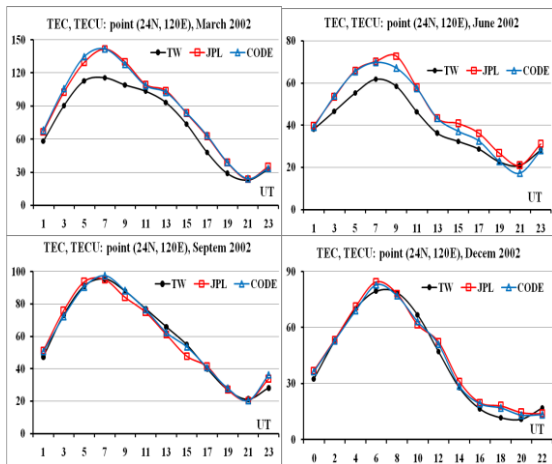


Figure 2: Comparison of model and observational TEC for the Taiwan model near to a maximum of solar activity.

Seasonal course of TEC at the given latitude and the full conformity of model and observational TEC for autumn and winter months is perfectly seen. In the spring and in the summer, the model underestimates values. Range of the root mean square (RMS) deviation makes 4-14 TECU, the relative RMSD makes 6-18 %. On Fig. 3, results for a minimum of solar activity are yielded. Additionally, values of IGS are shown by asterisks.

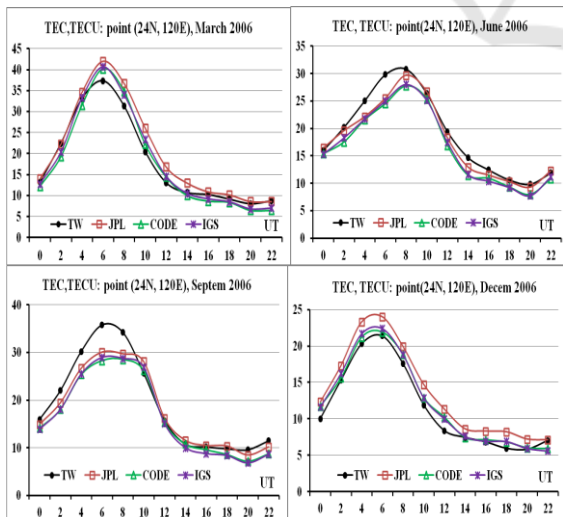


Figure 3: Comparison of model and observational TEC for the Taiwan model near to a minimum of solar activity.

It is seen that values of TEC can be in 2-3 times less, than in a maximum of solar activity. The model can both to underestimate and to overestimate the observational values. The range of absolute deviations has made 1-10 TECU. Absolute (σ , TECU) and relative (σ , %) RMSD are presented to Tab. 2 for four months of three years.

Table 2: Absolute and relative RMS deviations for the model (Kakinami, 2009).

σ , TECU	Mar	Jun	Sep	Dec
2002	13.5	8.0	3.5	4.0
2006	3.0	1.7	2.6	2.2
2010	5.6	2.8	5.9	5.6
σ , %	Mar	Jun	Sep	Dec
2002	15.8	17.2	6.0	8.9
2006	14.7	9.5	14.6	16.2
2010	24.3	16.3	26.2	24.3

If to compare these results with 50 % - estimation for the model (Klobuchar, 1987) then improving in 2-5 times may be got. Important property of the model is dependence of TEC on a daily index. The previous Figures 2 and 3 showed results for medians. The following Fig. 4 gives comparison of daily model and experimental values for August 2002.

Good correspondence of dynamics of TEC variations is seen. That proves to be true by quantitative estimations of absolute deviations 6.4 TECU, absolute RMS deviations 8.3 TECU and relative RMSD 16.4 %. These results show high efficiency of the model and a way of its construction. It can be used for validation of other models.

One more aspect of use of models is connected with reconstruction of TEC values for those periods when there were no regular measurements of TEC (before 1998). The possibility of such reconstruction is illustrated on Fig. 5 according to GPS measurements at the Taiwan station in the morning since September 1996 till August 1997 (Wu et al., 2004). Icon TEC represents measurements, TW - values of the Taiwan model.

It is seen that results are satisfactory as a first approximation. They give representation also about possibilities of forecast forward.

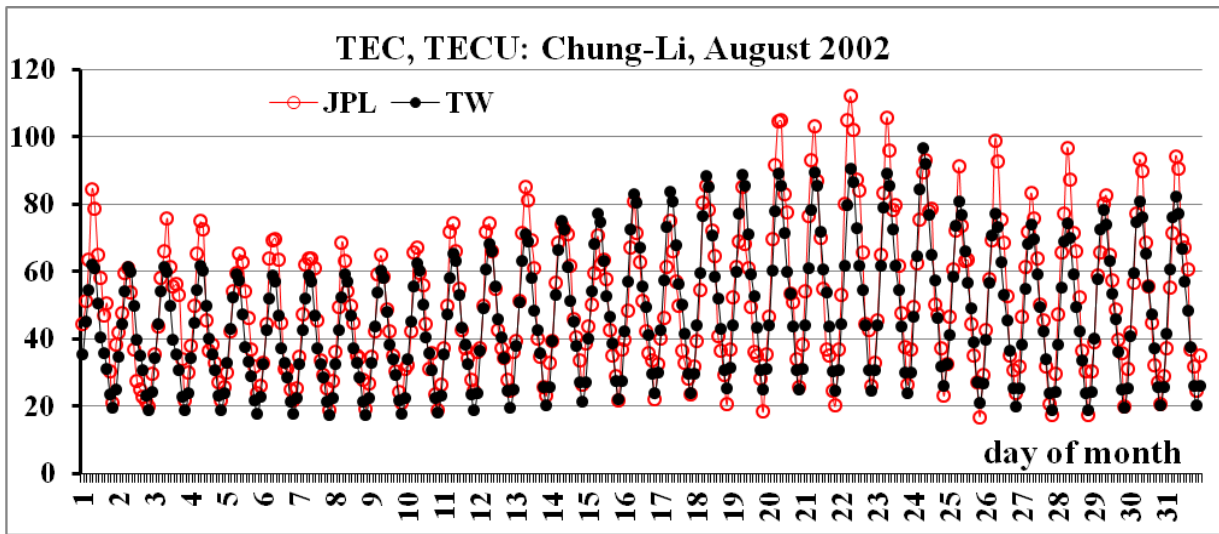


Figure 4: Comparison of daily model and experimental TEC for August 2002.

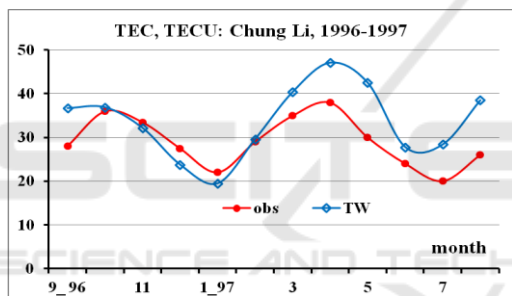


Figure 5: Comparison of model and observational TEC in years 1996-1997.

The Neustrelitz Global Model (NGM) unlike the Taiwan model is global one (Jakowski et al., 2011). Except the TEC model, it includes models of other parameters (NmF2, hmF2) (Hoque and Jakowski, 2011, 2012). Authors of this model have fulfilled own validation however it is not enough for certain conclusions about efficiency of their model. Results of more extensive validation are given in (Maltseva et al., 2013c) for a middle-latitude region and in (Maltseva et al., 2013b) for low-latitude area in which the greatest advantages were expected. Results of additional validation for low-latitude stations Niue and Sao Luis are given on Fig. 6, for high-altitude stations are given on Fig. 7.

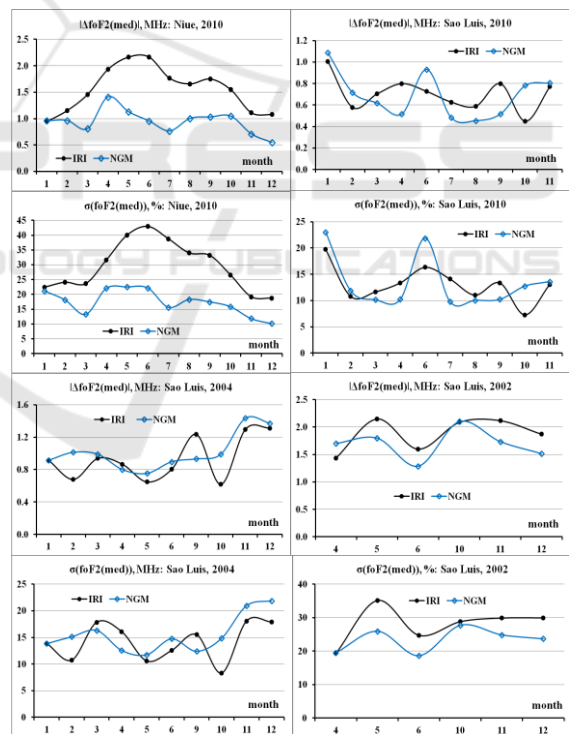


Figure 6: Cases of the NGM model advantage at definition of foF2 (two low-latitude stations, 2010, 2004, 2002).

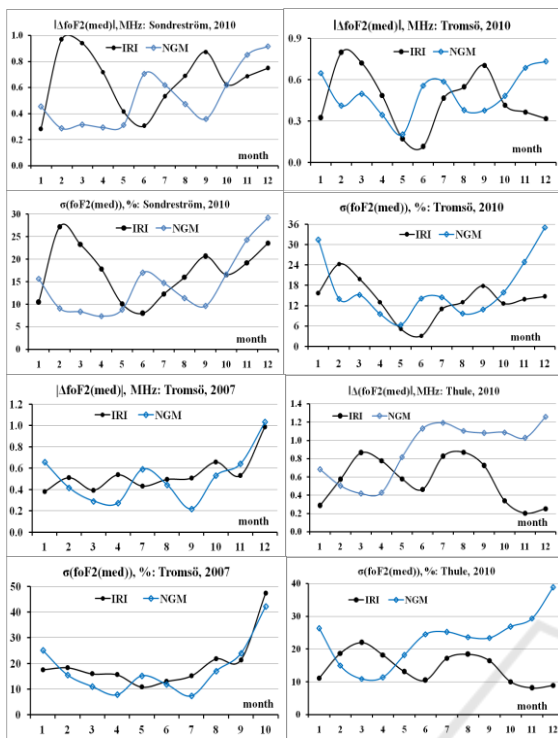


Figure 7: Cases of the NGM model advantage at definition of foF2 (three high-altitude stations, 2010, 2007).

In these cases, periods of the NGM model advantages are seen, however the major statistics on all regions shows that the NGM model not always yields the best results, than the IRI model. Discrepancy between radio occultation and ionosonde values of NmF2 may be one of the reasons why insert of great number of radio occultation measurements has not led to improvement of the NGM model, e.g. (Hajj and Romans, 1998; Tsai and Tsai, 2004). Nevertheless, it can be recommended for use in low- and high-latitude areas.

Process of model development continues constantly that is additional confirmation of an urgency of this process. The latest model is the model of authors (Mukhtarov et al., 2013a, b). It, on the one hand, is the most physically proved, on the other hand, according to estimates of authors, their model is two times more exact, than the NGM model. In papers (Mukhtarov et al., 2013a, b), not only the TEC model is developed, but also model of its error (Mukhtarov et al., 2013b). Difference from the NGM model is the consideration not only components, caused by sunlight, but also the regular wave structure of the tidal nature influencing from the lower atmosphere. The model is constructed

according to the CODE map for 1999-2011. As the starting parameter, not only coefficient F10.7 is chosen, but also its linear velocity of change K_F . It is one more difference of this model from all previous options. For all array of the used data, the following estimates are obtained: mean (systematic) error $ME=0.003TECU$, at such ME, root of mean square error (RMSE) and an error of a standard deviation (STDE) were equal and have made $RMSE=STDE=3.387TECU$. These estimates are compared to estimates for the TEC(NGM) model (Jakowski et al., 2011): $ME=-0.3TECU$, $RMSE=7.5TECU$. Thus, the Bulgarian model has a smaller error in two times. However it is worth to note that both models are climatological, i.e. they describe a mean state in quiet geomagnetic conditions, and the difference in number of coefficients (12 against 4374) is underlined. Authors of (Mukhtarov et al., 2013a) absolutely validly do not consider a great number of coefficients as a model deficiency because these coefficients are calculated once, however they are inaccessible. Coefficients of the TEC(NGM) model are published and may be used by any user. In turn, we can note that there are "tails" in an error distribution of any model. It is important to determine, what latitudinal areas and to what conditions of solar activity they concern. As any model cannot work equally well in all latitudinal areas and meet the possible requirements, validation of models does not cease to be an actual problem. These requirements are connected with limitation of approaches, the used data, distinction of physical processes.

Thus, it is possible to specify major progress in modeling of parameter TEC: occurrence of various models allows us to compare and use them at forecast of TEC for any level of solar activity. It is especially important because values of solar spots and parameter F10.7, and also geomagnetic coefficients of K_p , Dst, AE are well enough predicted (e.g. Pesnell, 2012; Tobiska et al., 2013).

4 DEFINITION OF FoF2 ON CURRENT VALUES OF TEC

Definition of foF2 on current values of TEC in the this paper is based on use of median of the equivalent slab thickness of the ionosphere τ . Empirical models of τ have appeared earlier, than empirical models of TEC. Definition of TEC under formula $TEC=\tau*NmF2$, where the independent empirical model of τ should be used, was one of

main applications of the τ model. NmF2 is possible to take from the IRI model or any another. The simple relation for $\tau = \text{TEC}/\text{NmF2}$ shows that τ is width of a slab in the form of a rectangle with constant concentration NmF2. For definition of TEC and NmF2, the $\tau(\text{IRI})$ model was traditionally used (e.g. Houminer and Soicher, 1996; Gulyaeva, 2003) though it also is not empirical in the same sense in what the TEC(IRI) model is not empirical model of TEC. On the basis of expression $\text{foF2} = \text{foF2}(\text{IRI}) * \text{SQRT}(\text{TEC}(\text{obs})/\text{TEC}(\text{IRI}))$, GIM-TEC adaptive ionospheric weather assessment and forecast system was constructed (Gulyaeva et al., 2013). It is easy to show that value which can be designated $\tau(\text{obs}, \text{IRI})$ is used in this case. It means that model values of NmF2 and the observational values of TEC are used at definition of $\tau(\text{obs}, \text{IRI})$. It differs as from $\tau(\text{IRI}, \text{IRI})$, and from $\tau(\text{obs}, \text{obs})$ which are designated $\tau(\text{IRI})$ and $\tau(\text{obs})$ for brevity of records. Papers (Maltseva et al., 2012a, b) are devoted results of use of median $\tau(\text{med})$ from values $\tau(\text{obs})$. Empirical models of ionospheric parameters are known to include median or mean values hence they characterize a mean state, close to the quiet. Advantage of median $\tau(\text{med})$ is that it allows to determine foF2 on current values of TEC. These foF2 values differ from averages and are closer to the real. In paper (Maltseva et al., 2012a), it is shown that the median $\tau(\text{med})$ allows to determine foF2 during disturbances or to fill gaps of the foF2 data. The estimate of efficiency of use of values τ is done by means of calculation of deviations $|\Delta\text{foF2}|$ of calculated foF2 from the observational ones. The observational values of TEC form the whole array: JPL, CODE, UPC, ESA, La Plata, IONOLab TEC, RAL and others. To each of these values, the various values of τ correspond. The example of τ behavior for the JPL map is shown on Fig. 8 for the Juliusruh station for April 2000 (near to a maximum of solar activity) and April 2009 (near to a minimum of solar activity).

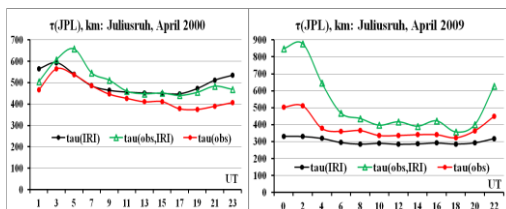


Figure 8: An example of comparison of τ for various options of TEC and NmF2.

Example of the foF2 definition by means of various τ is given on Fig. 9 together with

experimental values of TEC for the JPL map. These values are shown together with medians. This picture specifies presence of disturbance.

Tab. 3 shows results of $|\Delta\text{foF2}|$ calculation for four global maps JPL, CODE, UPC, ESA. These are monthly average values of deviations for the instantaneous quantities foF2(ins). Values of $|\Delta\text{foF2}|$ for $\tau(\text{IRI})$ are given for comparison.

The table illustrates the most general regularities: the greatest deviations are proper $\tau(\text{IRI})$ in the initial model, the little smaller deviations correspond to $\tau(\text{obs}, \text{IRI})$. The best conformity is given by median of $\tau(\text{obs})$. From four maps, the best conformity concerns the JPL map in this case. And though it gives the best conformity in most cases, there are conditions and regions in which the best conformity can be given and by other maps. More often it is CODE, sometimes - UPC. And even there was a station (Sao Luis) for which the best conformity is given by the ESA map in certain cases. The huge statistics of calculations for more, than 30 stations and 10 years, shows that deviations of the calculated frequencies from the observational values have the greatest quantity for $\tau(\text{IRI})$, the least - for $\tau(\text{obs})$, i.e. $\tau(\text{med})$. Deviations for $\tau(\text{obs}, \text{IRI})$ lie between them, closer to $|\Delta\text{foF2}|$ for $\tau(\text{IRI})$ more often. New results, including the data for values IGS, are given in Tab. 4 for high- and low-latitude stations which determine boundaries of values $|\Delta\text{foF2}|$, because values for middle-latitude stations are always less. Values, averaging for 2013, are given.

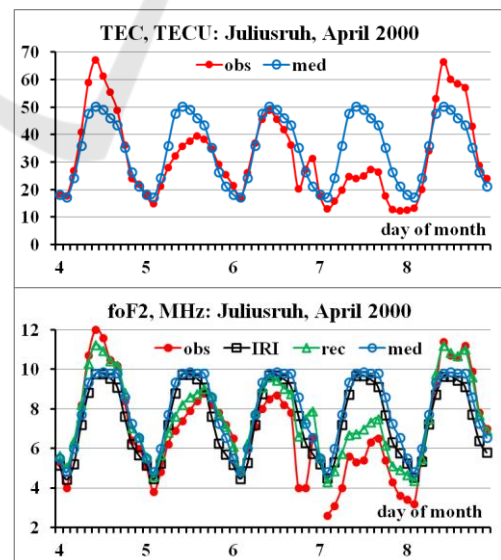


Figure 9: An example of use of median of τ for definition of foF2.

Table 3: Deviations $|\Delta foF2|$ for various options of τ definition.

$ \Delta foF2 $, MHz	April 2000		April 2009	
	$\tau(IRI) \rightarrow$	1.034	$\tau(IRI) \rightarrow$	0.554
	τ (obs,IRI)	$\tau(obs)$	τ (obs,IRI)	$\tau(obs)$
JPL	0.660	0.452	0.497	0.205
CODE	0.677	0.484	0.501	0.222
UPC	0.731	0.544	0.472	0.237
ESA	1.013	0.907	0.496	0.242

Table 4: Correspondence between experimental and calculated foF2 according to three stations.

$ \Delta foF2 $	$\tau(IRI)$	$\tau(obs, IRI)$					$\tau(obs)$				
		station	IRI	JPL	CODE	UPC	ESA	IGS	JPL	CODE	UPC
Thule	0.82	0.71	0.75	0.71	0.75	0.71	0.41	0.45	0.41	0.45	0.41
Longyear	0.69	0.61	0.67	0.59	0.63	0.62	0.40	0.49	0.38	0.43	0.41
Niue	2.19	2.09	2.16	2.15	2.13	2.13	1.01	1.10	1.09	1.06	1.04

Value for IGS is inscribed in the general statistics and more often there is a little above, than a value for the best map. It is worth to note that the proximity of values $|\Delta foF2|$ for various maps testifies that τ is good calibration coefficient for TEC.

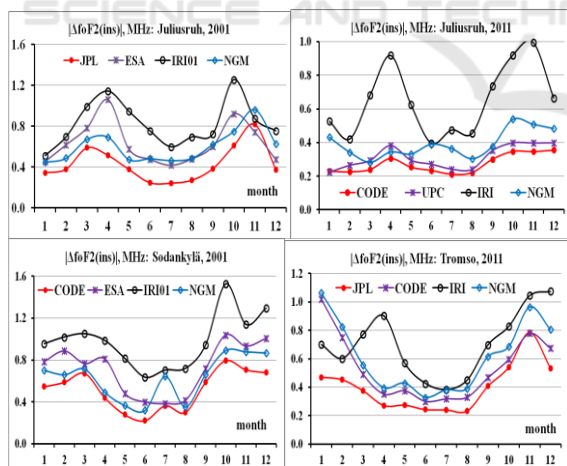


Figure 10: Comparison of results of foF2 definition with use of various τ .

In connection with such results, there is a question on empirical model of τ . One of possibilities is to pay attention to the NGM model which allows to calculate NmF2(NGM) and TEC(NGM). Having values NmF2(NGM) and

TEC(NGM), it is possible to calculate values of the equivalent slab thickness of the ionosphere $\tau(NGM) = TEC(NGM)/NmF2(NGM)$. The purpose is to estimate, how much the model $\tau(NGM)$ is closer to $\tau(obs)$ than $\tau(IRI)$. Such estimate is done by comparison of instantaneous values $|\Delta foF2(ins)|$. For the NGM model, values of foF2(ins) are obtained from values TEC(CODE) with use of $\tau(NGM)$. On Fig. 10, examples of comparison of critical frequencies for two global maps are given ("best" and "worst" from the point of view of definition of foF2 in each specific case) and two models (IRI and NGM) for middle-latitude and two high-altitude stations in the conditions of various solar activity.

It is seen that near to a maximum of activity (2001) the NGM model yields the best results than the IRI model and the ESA map. In the conditions of low activity (2006) at middle-latitude station, it yields results, close to IRI. At high latitudes, the NGM model gives major deviations in winter and autumn, and it is seen that the CODE map yields the worst results in these cases. At an increase of solar activity in 2011 and the corresponding increase of the TEC, the NGM model again starts to yield results, the best than the IRI model. Thus, in most cases $\tau(NGM)$ provides results, the best than $\tau(IRI)$, however its deviations do not come nearer anywhere to the values given by $\tau(JPL)$. In the conditions of a minimum of activity, the NGM model has no advantages to low-latitude stations.

As a whole, it is possible to tell that τ (NGM) may carry out a role of the empirical model of τ . At use of other map instead of the CODE map, probably, results would be better.

4 N(h)-PROFILE S OF THE IONOSPHERE AND VALUES OF TEC

As it is known, conditions in the ionosphere are determined by distribution of concentration, or N(h)-profile. N(h)-profile can be divided into three parts: bottom side, topside and plasmaspheric. The bottom side is determined by the experimental critical frequency foF2. The topside is improved by means of the plasma frequencies measured on satellites, but there is a residual of TEC. It is possible to use coefficient K(PL) which is selected for the full conformity with the observational TEC. However there is no data for development and validation of the K(PL) model yet. Having such model, it will be possible even to improve determination of foF2. Details of use of TEC for determination of N(h)-profile to heights of navigation satellites are the following. In paper (Maltseva et al., 2013c), it has been shown that use of the plasma frequencies measured on satellites allows to improve the shape of the topside side. As a result, values of TEC for the several N(h)-profiles transiting through the critical frequency foF2 and a various combination of plasma frequencies are obtained: (1) satellite s1, (2) satellite s2, (3) both satellites s1 and s2. Two first options are realized in most cases. The third option is realized in case of simultaneous passage of two satellites over the given point. The illustration of obtained values of TEC is given for the Juliusruh station on Fig. 11. Simultaneous passages took place for 6 days specified in Tab. 5 in UT=13 and UT=23. Values for the initial IRI model are shown by black circles. Red circles show the observational values. Green triangles show values for the first option, by violet crosses - for the second one, blue asterisks – for the third case. Orange circles show TEC for the N(h)-profiles transiting through both plasma frequencies and adapting by coefficient K(PL). All values are given for four maps in decreasing order of values. This order is specified in Tab. 5.

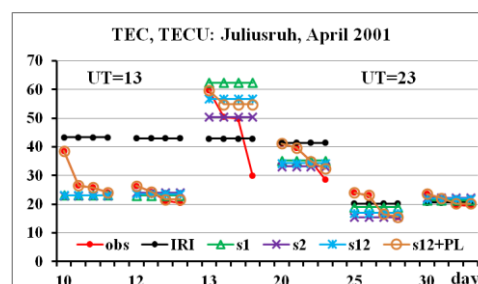


Figure 11: TEC, calculated for N(h)-profiles, transiting through the critical frequency foF2 and a various combination of plasma frequencies.

Table 5: Days, hours and names of maps in decreasing order of TEC for simultaneous passages of satellites over the Juliusruh station in April 2001.

day	hour	map			
10	13	ESA	JPL	UPC	CODE
12	13	JPL	UPC	CODE	ESA
13	13	JPL	CODE	UPC	ESA
20	13	JPL	UPC	CODE	ESA
25	23	UPC	JPL	ESA	CODE
30	23	JPL	UPC	CODE	ESA

Big difference between TEC for the corrected N(h)-profiles and TEC for the initial model, corresponding to quiet conditions, speaks about influence of disturbances. N(h)-profiles transiting through frequency of one of satellites, are close each other. That can testify both to "interchangeability" of profiles, and about their ambiguity. In most cases, orange circles coincide with red points. It testifies that the N(h)-profile, transiting through plasma frequencies of both satellites, provides the observational value of TEC. It is reached by selection of coefficient K(PL) shown on Fig. 12 also for four maps.

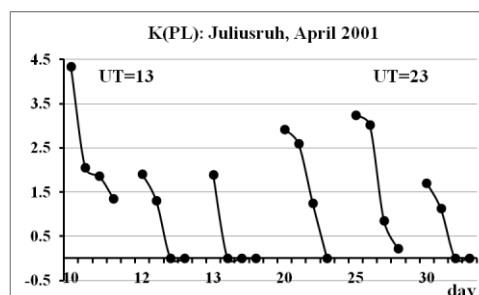


Figure 12: Behavior of coefficient K(PL) for four global maps of TEC in cases of simultaneous passages of satellites.

It is seen that values of $K(PL)$ decrease with decreasing $TEC(obs)$. Relation $K(PL) = 1$ specifies the full conformity of model TEC and $TEC(obs)$. It is obvious that it is possible to select the TEC value to which relation $K(PL) = 1$ corresponds. There are some cases with the negative value $K(PL) = -0.001$. They can be identified by misfit of orange and red circles on Fig. 13. It means that the $N(h)$ -profile, providing $TEC(obs)$, is not found. It occurs when TEC for $N(h)$ -profiles $s1$ exceed $TEC(obs)$.

The $N(h)$ -profiles corresponding to these TEC are given on Fig. 13.

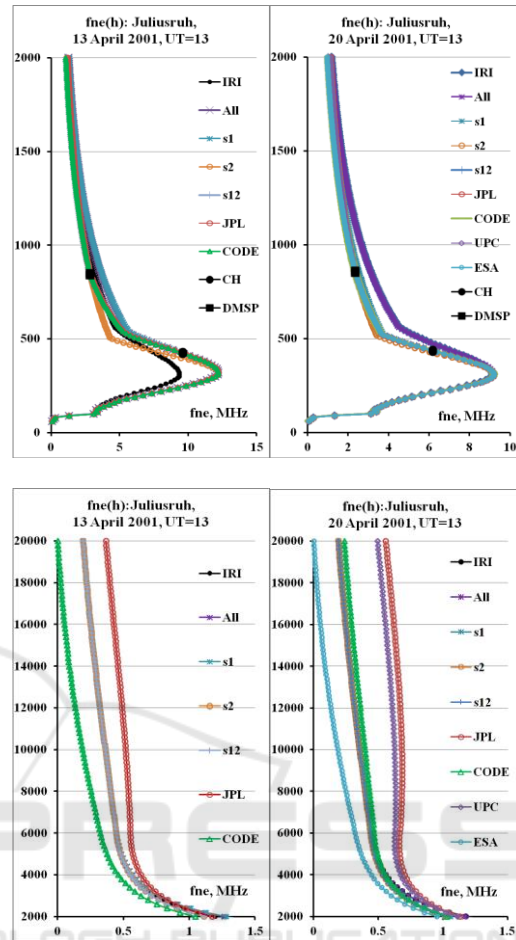
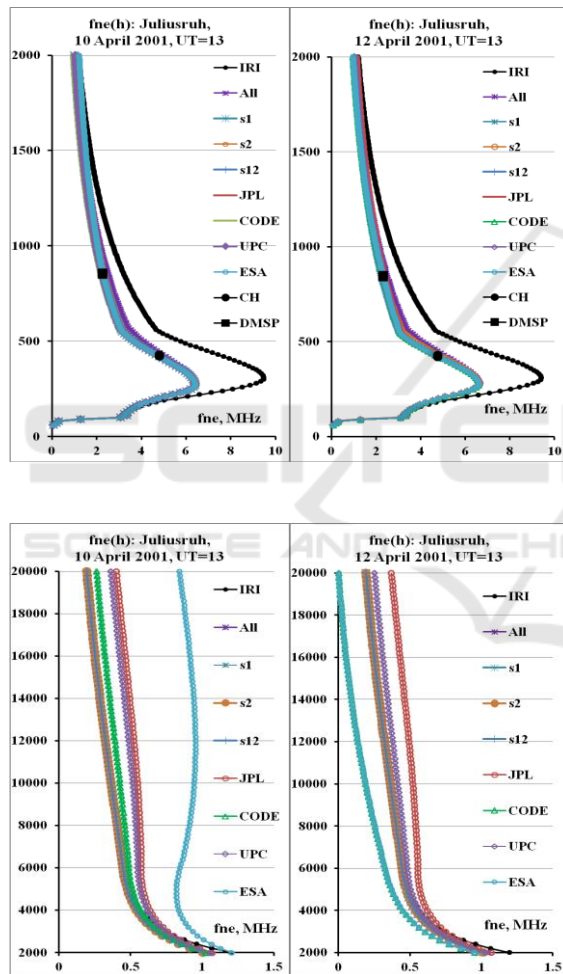


Figure 13: Topside and plasmaspheric parts of $N(h)$ -profiles corresponding various global maps of TEC .

4 CONCLUSIONS

In recent years, the TEC has become an important parameter to describe the state of the propagation medium. However, its use encounters certain difficulties associated with a variety of values. This diversity leads to ambiguity of parameters determined through TEC and models. This paper makes the following recommendations. 1. The best method of TEC modeling is the EOC. 2. To determine $foF2$, it is possible to use τ , which is a good calibration factor, including $\tau(NGM)$. 3. Using plasma frequencies measured on satellites allows us to construct $N(h)$ -profiles, closer to the real part in the topside part. 4. For full proximity of $N(h)$ -profiles with experimental $TEC(obs)$, we must enter the factor $K(PL)$, modifying plasmaspheric part of profile. Its value depends on the choice of $TEC(obs)$. In this regard, we can focus on IGS.

ACKNOWLEDGEMENTS

Author thanks organizations and scientists who are developing the IRI model, providing data of SPIDR, JPL, CODE, UPC, ESA, and Dr M. Hoque for detailed comments on the NGM model.

REFERENCES

- Arikan, F., Erol C.B., Arikan O., Regularized estimation of vertical total electron content from Global Positioning System data. 2003. *J. Geophys. Res.*, 108, A12, 1469, doi:10.1029/2002JA009605, 12p.
- Chen, K., Gao Y. Real-time precise point positioning using single frequency data. *Proceedings of IONGNSS 18th International Technical Meeting of the Satellite Division, Long Beach, CA, 2005, 1514-1523.*
- Goodman, J.M., 2005. Operational communication systems and relationships to the ionosphere and space weather. *Adv. Space Res.*, 36, 2241–2252.
- Gulyaeva, T.L., 2011. Storm time behavior of topside scale height inferred from the ionosphere-plasmasphere model driven by the F2 layer peak and GPS-TEC observations. *Adv. Space Res.*, 47, 913-920.
- Gulyaeva, T.L., Arikan F., Hernandez-Pajares M., Stanislawska I. 2013. GIM-TEC adaptive ionospheric weather assessment and forecast system. *J. Atm. Solar-Terr. Phys.*, 102, 329-340.
- Gulyaeva, T.L., Bilitza D., 2011. Towards ISO standard Earth ionosphere and plasmasphere model. In: *Larsen, R.J. (Ed.), New developments in the standard model. NOVA Publishers, USA, 11–64.*
- Gulyaeva, T.L., Stanislawska, I., 2008. Derivation of a planetary ionospheric storm index. *Ann. Geophys.*, 26, 2645–2648.
- Hajj, G.A., Romans L.J., 1998. Ionospheric electron density profiles obtained with the Global Positioning System: results from the GPS/MET experiment. *Radio Sci.*, 33, 175–190.
- Hernandez-Pajares, M., Juan, J. M., Orus, R., Garcia-Rigo, A., Feltens, J., Komjathy, A., Schaer, S. C., and Krankowski, A.: The IGS VTEC maps: a reliable source of ionospheric information since 1998. *J. Geod.*, 2009, 83, 263–275.
- Hernandez-Pajares, M., Juan, J.M., Sanz, J., 1997. High-resolution TEC monitoring method using permanent ground GPS receivers, *Geophys. Res. Lett.*, 24, 1643-1646.
- Hoque, M.M., Jakowski N., 2011. A new global empirical NmF2 model for operational use in radio systems. *Radio Sci.*, 46, RS6015, 1-13.
- Hoque, M.M., Jakowski N., 2012. A new global model for the ionospheric F2 peak height for radio wave propagation. *Ann. Geophys.*, 30, 797-809.
- Houminer, Z., Soicher H., 1996. Improved short-term predictions of foF2 using GPS time delay measurements. *Radio Sci.*, 31(5), 1099-1108.
- Ivanov, V.B., Gefan G.D., Gorbachev O.A., 2011. Global empirical modeling of the total electron content of the ionosphere for satellite radio navigation systems. *J. Atm. Solar-Terr. Phys.*, 73, 1703–1708.
- Jakowski, N., Hoque M.M., Mayer C. A new global TEC model for estimating transionospheric radio wave propagation errors, *Journal of Geodesy*, 2011, 85(12), 965-974.
- Jakowski, N., Sardon E., Engler E., Jungstand A., Klahn D., 1996. Relationships between GPS-signal propagation errors and EISCAT observations. *Ann. Geophys.*, 14, 1429-1436.
- Jakowski, N., Stankov S.M., Schlueter S., Klaehn D., 2006. On developing a new ionospheric perturbation index for space weather operations. *Adv. Space Res.*, 38, 2596-2600.
- Kakinami, Y., Chen C.H., Liu J.Y., Oyama K.-I., Yang W.H., Abe S., 2009. Empirical models of total electron content based on functional fitting over Taiwan during geomagnetic quiet condition. *Ann. Geophys.*, 27, 3321-3333.
- Klobuchar, J.A., 1987. Ionospheric time-delay algorithm for single-frequency GPS users. *IEEE Transactions on aerospace and electronic systems*. 1987AES-23(3), 325-331.
- Lastovicka, J. Are trends in total electron content (TEC) really positive? *J. Geophys. Res.: Space Physics*, 2013, 118, 3831–3835, doi:10.1002/jgra.50261.
- Lean, J., Emmert J.T., Picone J.M., Meier R. R. Global and regional trends in ionospheric electron content. *J. Geophys. Res.*, 2011, 116, A00H04, doi:10.1029/2010JA016378.
- Maltseva, O.A., Mozhaeva N.S, Zhbankov G.A., 2012a. A new model of the International Reference Ionosphere IRI for telecommunication and navigation systems. *Proceedings of the First International Conference on Telecommunications and Remote Sensing, Sofia, Bulgaria 29-30 August 2012, 129-138*, http://www.math.bas.bg/ursi/ICTRS2012_proceedings.pdf
- Maltseva, O.A., Mozhaeva N.S, Poltavsky O.S., Zhbankov G.A., 2012b. Use of TEC global maps and the IRI model to study ionospheric response to geomagnetic disturbances. *Adv. Space Res.*, 49, 1076-1087.
- Maltseva, O. A., Zhbankov G. A., Mozhaeva N.S., 2013a. Advantages of the new model of IRI (IRI-Plas) to study ionospheric environment. *Adv. Radio Sci.*, 11, 907–911, doi:10.5194/ars-11-1-2013.
- Maltseva, O.A., Mozhaeva N.S, T.V. Nikitenko, 2013b. Validation of the Neustrelitz Global Model according to the low latitude ionosphere. *Adv. Space Res.*, <http://dx.doi.org/10.1016/j.asr.2013.11.005>.
- Maltseva, O., Mozhaeva N., Vinnik E., 2013c. Validation of two new empirical ionospheric models IRI-Plas and NGM describing conditions of radio wave propagation in space. *Proceedings of Second International Conference on Telecommunications and Remote Sensing, Noordwijkerhout, The Netherlands, 11-12 July*, 109-118.
- Mukhtarov, P., Pancheva D., Andonov B., Pashova L., 2013a. Global TEC maps based on GNSS data: 1.

- Empirical background TEC model. *J. Geophys. Res.: Space Physics*, 118, 4594–4608, doi:10.1002/jgra.50413.
- Mukhtarov, P., Pancheva D., Andonov B., Pashova L., 2013b. Global TEC maps based on GNSS data: 2. Model evaluation. *J. Geophys. Res.: Space Physics*, 118, 4609–4617, doi:10.1002/jgra.50412.
- Mannucci, A. J., Wilson B. D., Yuan D. N., Ho C. H., Lindqwister U.J., Runge T.F., 1998. A global mapping technique for GPS-derived ionospheric total electron content measurements. *Radio Science*, 33(3), 565-582.
- Mukhtarov, P., Pancheva D., Andonov B., Pashova L., 2013. Global TEC maps based on GNSS data: 1. Empirical background TEC model. *J. Geophys. Res.: Space Physics*, 118, 4594–4608, doi:10.1002/jgra.50413.
- Pesnell, W.D. Solar Cycle Predictions (Invited Review), *Solar Phys*, 2012, 1-26, DOI 10.1007/s11207-012-9997-5.
- Sardon, E., Rius A., Zarraoa N., 1994. Estimation of the receiver differential biases and the ionospheric total electron content from Global Positioning System observations. *Radio Sci.*, 29, 577-586.
- Schaer, S., Beutler G., Mervart L., Rothacher M., Wild U., 1995. Global and regional ionosphere models using the GPS double difference phase observable. *IGS Workshop, Potsdam, Germany, May 1995*, 1-16.
- Tobiska, W. K., D. Knipp, W. J. Burke, D. Bouwer, J. Bailey, D. Odstrcil, M. P. Hagan, J. Gannon, and B. R. Bowman, 2013. The Anemomilos prediction methodology for Dst. *SpaceWeather*, 11, 490–508, doi:10.1002/swe.20094.
- Tsai, Lung-Chih, Tsai Wei-Hsiung, 2004. Improvement of GPS/MET Ionospheric Profiling and Validation Using the Chung-Li Ionosonde Measurements and the IRI model. *Terr. Atmos. Ocean. Sci.*, 15(4), 589-607.
- Wu, Chin-Chun, Fryb C.D., Liuc J.-Y., Lioud K., Tseng C.-L., 2004. Annual TEC variation in the equatorial anomaly region during the solar minimum: September 1996–August 1997. *J. Atm. Solar-Terr. Phys.*, 66, 199–207.